ACS APPLIED MATERIALS & INTERFACES

Research Article

www.acsami.org

Light-Responsive Iron(III)–Polysaccharide Coordination Hydrogels for Controlled Delivery

Giuseppe E. Giammanco, Christopher T. Sosnofsky, and Alexis D. Ostrowski*

Center for Photochemical Sciences and Department of Chemistry, Bowling Green State University, Bowling Green, Ohio 43403, United States

Supporting Information

ABSTRACT: Visible-light responsive gels were prepared from two plant-origin polyuronic acids (PUAs), alginate and pectate, coordinated to Fe(III) ions. Comparative quantitative studies of the photochemistry of these systems revealed unexpected differences in the photoreactivity of the materials, depending on the polysaccharide and its composition. The roles that different functional groups play on the photochemistry of these biomolecules were also examined. Mannuronic-rich alginates were more photoreactive than guluronic acid-rich alginate and than pectate. The microstructure of alginates with different mannuronate-to-guluronate ratios changed with polysaccharide composition. This influenced the gel morphology and the photoreactivity. Coordination hydrogel beads were prepared from both Fe–alginate and Fe–pectate. The beads were stable carriers of molecules as diverse as the dye Congo Red, the vitamin folic acid, and the antibiotic chloramphenicol. The photoreactivity of the hydrogel beads mirrored the photoreactivity of the polysaccharides in solution, where beads prepared with alginate released their cargo faster than beads prepared with pectate. These results indicate important structure–function relationships in these systems and create guidelines for the design of biocompatible polysaccharide-based materials where photoreactivity and controlled release can be tuned on the basis of the type of polysaccharide used and the metal coordination environment.

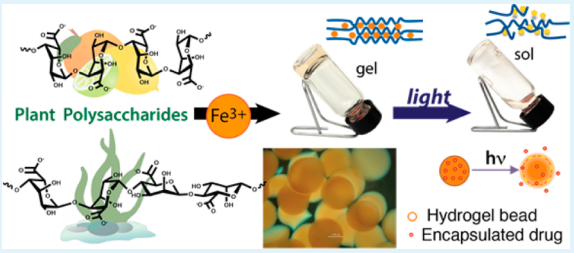

KEYWORDS: *photochemistry, stimuli-responsive materials, coordination hydrogels, polysaccharides, controlled release*

1. INTRODUCTION

Hydrogels are versatile materials capable of absorbing high amounts of water and can adjust mechanical properties upon environmental changes, such as temperature, pH, or ionic strength. These unique characteristics make them common candidates for applications in biology and biomedicine, where they can be used in tissue engineering,[1−5] regenerative medicine,[2,6−8] drug delivery,[9−12] and sensing.[13,14] In most hydrogels, the polymer chains are chemically cross-linked, which creates a covalent network able to swell or shrink but restrained to the bond lengths of its constituents.

In order to expand the functionality of hydrogels and obtain more advanced, highly homogeneous, and self-healing materials, one approach is to use more dynamic noncovalent interactions with polyvalent metal ions for the cross-linking.[15,16] Ionic polysaccharides, such as alginate, for example, can form cross-linked hydrogels with Ca^{2+} and have proven to be biocompatible materials suitable for biomedical applications, such as cell support,[17−19] cell delivery,[20] and drug encapsulation and delivery.[21−24] In addition to Ca^{2+}, transition metal ions like Fe^{3+} have been shown to form hydrogels with alginate.[17,24,25] The coordination bond formed with transition metal ions creates a covalent contribution not seen with ions like calcium.[26] The dynamic nature of the metal-coordination bond allows for extra functionality, where active bond making-and-breaking gives rise to new stabilities and macroscopic properties of the resulting metal-coordination materials.[7,27,28] Specifically, these dynamic bonding interactions impart new mechanical properties to the materials that can be controlled by changing the metal-coordination environment.[27,29−31]

Narayanan et al. reported the formation of hydrogel materials prepared from iron ions and alginate.[25] The coordination hydrogels are photosensitive when small amounts of a sacrificial hydroxy carboxylate (SC), lactic acid, are present.[25] These authors described a gel–sol transition in this system due to the photoreduction of the Fe^{3+} to ferrous ions, which no longer serve as cross-linkers for the biopolymer. The concomitant decarboxylation of the sacrificial molecule (lactic acid) is also observed.[25] A carboxylate-containing polysaccharide—oxidized glucomannan from konjac—has also been shown to bind to Fe^{3+} and undergo physical changes upon broad-band visible light irradiation.[32]

Although some reports have been made regarding the photoresponsive behavior of iron–polyuronate coordination gels,[25,32] there are no records of the quantitative study of their photochemistry and the mechanism involved. Furthermore, the effect that the composition of the polysaccharide has on the photoreactivity has not been taken into account, and the

Received: October 1, 2014
Accepted: January 15, 2015
Published: January 15, 2015

DOI: 10.1021/am506772x
ACS Appl. Mater. Interfaces 2015, 7, 3068−3076

photochemistry of pectic polysaccharides coordinating iron has not been previously studied.

We report here newly formulated photoresponsive coordination hydrogels from iron(III) ions and the polysaccharides poly[guluronan-*co*-mannuronan] (alginate) and poly-[galacturonan] (pectate), the structures of which are presented in the Supporting Information (Figure S1). No extra component, e.g., a sacrificial α-hydroxycarboxylate, was required in order to provide these materials with photoreactivity. Physical changes in the Fe−polysaccharide gels were observed upon irradiation with visible (405 nm) LED light (Figure 1). We also describe detailed investigations of the

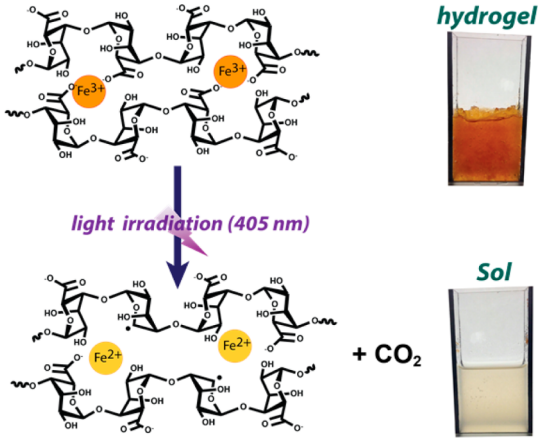

Figure 1. Physical and chemical changes in Fe^{3+}−pectate gels upon visible light irradiation.

quantitative photochemistry of these systems, since understanding these processes is necessary to ensure that a consistent, controlled response can be realized in a clinical application. This is especially important for alginate-based materials, where the source of the alginate influences the relative guluronate (G) and mannuronate (M) block composition as well as the molecular weight.

These results provide guidelines for actual application of the metal-coordination materials, where mechanical properties can be changed upon irradiation. Understanding the dependence of the photoreactivity on the composition of the polysaccharide allows one to design materials with specific, light-controlled properties in different environments (e.g., pH, redox) for a variety of biological applications, including tissue engineering and drug delivery.

2. EXPERIMENTAL SECTION

2.1. Materials. Low-viscosity sodium alginate from brown algae, M_v 45 000 g/mol (lot A112), coded as "alginate" for the purpose of this paper, was purchased from Sigma-Aldrich and used as received. Poly-D-galacturonic acid 95%, M_w 25 000−50 000 g/mol (lot 81325), was purchased from Sigma-Aldrich and prepared as the sodium salt by neutralization with NaOH. This material is referred to as "pectate". Medium-viscosity alginate (alginate-MV) and high-guluronate alginate (alginate-MVG), product codes IL-6F and IL-6G, respectively, were kindly supplied by Kimica Corp. Alginic acid (Lot 3REOH) was purchased from Tokio Chemical Industry Co., Ltd., and prepared as the sodium salt by neutralization with base (alginate-AA). Ferric chloride hexahydrate (98%), was purchased from Fluka and used as received; only freshly prepared solutions from this reagent were used. All other reagents were used as received.

2.2. Methods. *2.2.1. Synthesis of Acetylated PUA's.* In a general experiment the polyuronic acid sodium salt (1 g, 5 mmol) is suspended in 30 mL of cold distilled water and then 3 M NaOH is added to adjust the pH to 8. The reaction mixture is then placed in an ice bath and stirred for 10 min before adding acetic anhydride (1 g, 9.6 mmol). The mixture is taken from the ice bath and heated to reflux temperature for 5 min. The resulting solution is then allowed to cool before adding enough 0.1 M HCl to cause the product to precipitate (pH 2). Finally, 8 mL of ethanol is added and the mixture is centrifuged three times, washing the product with ethanol in the case of alginate and 2-propanol in the case of pectate. The degree of acetylation was calculated from the ^{1}H NMR data (Supporting Information, Figures S2 and S3). For alginate, this was done by comparing the area of the peak at 1.87 ppm, corresponding to the CH_3COO- protons, with the sum of the areas of the peaks at 5.19 ppm, corresponding to the proton G1, and the peaks at 4.67 and 4.61 ppm, corresponding to the protons MM1 and MG1, in the spectrum of the polysaccharide.[33] In the case of pectate, the area of the new peak is compared with that of the peak at 5.04 ppm, corresponding to the proton at the anomeric carbon.

2.2.2. Synthesis of Carboxymethylated PUA's. In a general procedure, the polyuronic acid sodium salt (1 g, 5 mmol) is suspended in 20 mL of cold distilled water and the mixture is stirred vigorously before carefully adding 3 equiv of NaOH to yield a bright yellow clear solution. Then, 2 equiv of monochloroacetic acid (MCA) is slowly added and the mixture is stirred for 3 h in a water bath at 70 °C. The reaction mixture is cooled down and the product is precipitated with 2 volumes of ethanol, filtered, and washed twice with 20 mL of a boiling mixture of ethanol in water 25% by weight. The degree of substitution was calculated from the ^{1}H NMR spectrum, according to the area of the singlet around 4.02 ppm, corresponding to the protons of the glycolic methylene (Supporting Information, Figures S4 and S5).

2.2.3. Synthesis of Carboxymethylated Starch. This synthesis was performed by a modification of a method reported in the literature.[34] Starch (1.0 g) is suspended in 25 mL of cold water and stirred at 50 °C. Then, 2.5 equiv of NaOH is added dropwise and the solution is stirred for 2 h. After this time, 2 equiv of MCA is slowly added and the reaction is stirred for 3 h more, after which the reaction is cooled and poured into 2 volumes of ethanol to precipitate the product. The degree of substitution was calculated from the integral of the peak around 4.04 ppm in the ^{1}H NMR spectrum (Supporting Information, Figure S6).

2.2.4. Hydrolysis of Polyuronic Acids. The hydrolysis was performed according to the method reported in the literature.[35] Briefly, 300 mg of the polyuronate was dissolved in a 1.5% H_2O_2 solution and stirred at 50 °C for 5 h. After this time, samples were allowed to cool, and the product was precipitated by addition of ethanol, centrifuged, and lyophilized.

2.2.5. Preparation of Iron(III)−PUA Complexes in Solution. The polyuronic acid sodium salt (0.1 g, 0.5 mmol) is suspended in 10 mL of a 0.9 mM $FeCl_3$ solution and stirred vigorously until complete dissolution. Samples are protected from room light during dissolution and handling, and they are exposed only to red light before the irradiation experiments.

2.2.6. Preparation of Iron(III)−PUA Hydrogel Beads. In a general experiment, a 1% w/v solution of the Na−PUA was slowly added dropwise from a syringe with a 25-gauge needle to a 0.1 M solution of $FeCl_3$. Beads were kept in the setting solution for 2 h before being washed twice with distilled water. The nearly spherical beads were then kept in distilled water at room temperature for 24 h, changing the medium three times during this period. For encapsulation experiments, the desired amount of the compound to be encapsulated (1.5 mg for Congo Red and 8 mg for chloramphenicol and folic acid) was dissolved in 1 mL of the polymer solution before dropping it on the iron solution.

2.2.7. Phototriggered Release from Iron(III)−PUA Beads. The loaded hydrogel beads (10 beads each) were placed inside a 1 cm path length quartz cuvette, and then 2 mL of aqueous release medium was added. Beads were irradiated by using a LED source with a power of 50 mW at 405 nm. A 1 mL aliquot of the release medium was used for measuring the absorbance before and after each irradiation period, after which the aliquot was poured back in the irradiation cuvette. The

DOI: 10.1021/am506772x
ACS Appl. Mater. Interfaces 2015, 7, 3068−3076

Scheme 1. Simplified Photochemical Reaction of Fe^{3+}−Carboxylates upon Irradiation with Visible Light

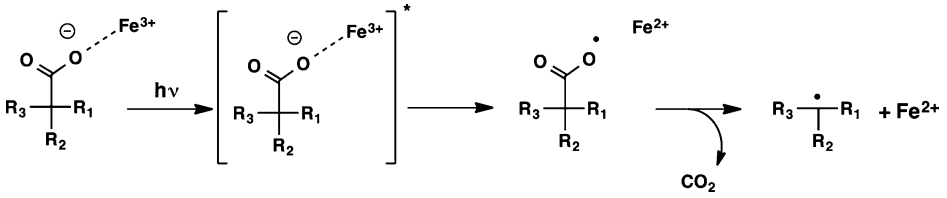

release process was screened by the increase in absorbance at the maximum wavelength for each host compound, i.e., 499 nm for Congo Red, 268 nm for folic acid, and 278 nm for chloramphenicol. The overall percent release was calculated on the basis of the amount of cargo released after complete dissolution of the beads.

2.2.8. Stability of Iron(III)−PUA Hydrogel Beads. In a general experiment, hydrogel beads loaded with Congo Red were placed in a 32-well plate containing 0.5 mL of the release medium. The plate was incubated at 37 °C in a Biotek ELx808 plate reader and the absorbance at 405 nm was measured every 15 min.

2.2.9. Solution Photochemistry. The photochemistry of the Fe^{3+}−polysaccharides was studied on samples that were 50 mM—by anhydroglucose unit—in the polysaccharide and 0.9 mM in the metal. Same concentrations of carboxylate and metal were used for experiments with other carboxylic acids, while for the experiments with sacrificial carboxylates, these were added in order to have a final concentrations of 20 mM. The absorbance spectrum of each sample was measured every 30 s of irradiation at 405 nm (high-power LED light source, Thor Laboratories). The quantum yield of the photoreaction (Φ) can be defined as the ratio of the moles of photoproduct per mole of photons absorbed by the sample, as shown in eq 1.

$$\Phi = \frac{\text{moles of photoproduct}}{\text{moles of photons absorbed}} \quad (1)$$

In our case, the photoproduct of interest was the Fe^{2+}, so the quantum yields are reported relative to the photoreduction of the metal according to eq 2

$$\Phi_{Fe(II)} = \frac{n\text{Fe(II)}}{I_0(1 - 10^{-\text{Abs}})} \quad (2)$$

where nFe(II) are the moles of ferrous iron generated after a given irradiation time, I_0 is the moles of photons incident on the sample during that time, and Abs is the absorbance of the sample at the irradiation wavelength. The amount of Fe^{2+} was quantitated by recording the absorbance of the 1,10-phenathroline complex at 510 nm. The intensity of the light source I_0 was determined by potassium ferrioxalate actinometry.

2.2.10. Solid State Photochemistry. Samples were prepared by suspending 0.1 g (0.5 mmol) of the PUA sodium salt in a 12.5 mM $FeCl_3$ solution and sonicating the resulting gelatinous mixture. Once the gels were obtained, they were lyophilized in the dark for 24 h. The resulting dark yellow solid was used for preparing KBr pellets that were 5% by weight in the sample. Absorbance of the pellets was studied by FTIR before irradiation and then after every 20 s of irradiation at 405 nm (50 mW). A stream of N_2 was maintained inside the sample chamber during the whole experiment.

2.2.11. Capillary Viscometry. Viscosity measurements of polysaccharide solutions (1.0 g/L) were carried out in a 0.1 M NaCl solution at 25 °C in an Ubbelohde viscometer (Cannon Instrument Co., 9721-N50, size 1-J337). The flow time was measured at five different polymer concentrations; each measurement was done at least three times.

For the titration experiments with iron, different amounts the Fe^{3+} solutions were mixed with a fix amount the polysaccharide solutions, so the final concentration of the Na−PUA was 1 g/L.

Changes in viscosity upon irradiation were studied for samples prepared by adding enough $FeCl_3$ to have a Fe:carboxylate ratio of 1:0.46. A total volume of 15 mL was irradiated inside the viscometer and the flow time was measured after each irradiation step.

For exhaustive irradiation experiments, polysaccharide solutions were mixed with ferric chloride solutions in order to get gels that were 50 mM in the PUA and 25 mM in the metal. Metallogels were irradiated at 405 nm until complete dissolution and deferrated with sodium ethylenediaminotetraacetate (EDTA), and the polysaccharide was precipitated with ethanol, washed, and lyophilized.

2.2.12. Circular Dichroism (CD) Measurements. CD spectra were recorded in an AVIV 62DS circular dichroism spectrophotometer at 25 °C. Polysaccharide samples were dissolved in deionized water to a concentration of 0.8 mg/mL and centrifuged to remove insoluble particles. A minimum of two scans were recorded per sample, and readings were collected every 0.5 nm with an integration time of 1 s.

2.2.13. Nuclear Magnetic Resonance Spectroscopy (NMR). NMR spectra were recorded in a Bruker AvanceIII 500 MHz spectrometer. Samples were dissolved in D_2O and analyzed measurements were run at 27 °C.

When iron was present in the sample, demetalation was performed by adding enough EDTA to completely dissolve the sample, before precipitating the sodium form of the polysaccharide by addition of ethyl alcohol.

2.2.14. Infrared (IR) Spectroscopy. Measurements were performed using a JASCO FTIR-4000 equipped with a single reflection ATR accessory. For measurements in KBr pellets, the accessory was replaced for a sample holder, and transmission spectra were collected.

2.2.15. Ultraviolet−Visible Spectroscopy (UV−vis). The absorbance spectra were measured using a Shimadzu UV-2600 spectrophotometer with a resolution of 0.5 nm.

3. RESULTS AND DISCUSSION

3.1. Quantitative Photochemical Study. The photoreaction undergone by Fe^{3+}−carboxylates is one of the oldest photochemical reactions reported.[36,37] It is expected that the Fe^{3+}−polysaccharide system will undergo similar photochemistry to other iron carboxylates and hydroxycarboxylates, just like those observed during the cycling of iron by dissolved organic matter in natural waters,[38] or that reported for some photoactive siderophores.[39,40] In these iron carboxylate systems, the ferric iron complex absorbs light, forming a short-lived excited state,[41] which decays nonradiatively by an electron transfer from the ligand (carboxylate) to the metal center (Fe^{3+}). The metal gets reduced and the carboxylate radical loses CO_2, forming a carbon-centered radical, which is able to undergo further chemistry[42] (see Scheme 1).

In the Fe^{3+}−polysaccharide systems, the physical state of the sample depends on the concentration of the metal, where homogeneous solutions are observed at low iron concentrations and stable solid gels are formed at higher metal concentrations (Supporting Information, Figure S7). In order to keep homogeneity in the samples used for the photochemical studies, the concentration of Fe^{3+} for preparing the polysaccharide complexes was fixed to 0.9 mM; at this concentration of the metal, all the samples were below the gel point and the results were reproducible and comparable.

DOI: 10.1021/am506772x
ACS Appl. Mater. Interfaces 2015, 7, 3068−3076

The photochemistry in these systems can be studied by examining spectral changes by UV−vis, as the absorbance of the sample decreases when the initial Fe^{3+} is photoconverted to Fe^{2+} [Figures 1 and S8 (Supporting Information)]. The amount of ferrous iron can then be calculated from changes in absorbance on the shoulder around 350 nm, which can be assigned as a weak transition attributed to the ligand to metal charge transfer (LMCT) (Supporting Information, Figure S8). However, for the purpose of this paper, the amount of Fe^{2+} photoproduced was directly quantified by using the 1,10-phenanthroline method.

Photochemical conversion of the Fe^{3+}−alginate system was highly dependent on pH, where a low efficiency (quantum yield) at pH >6 was observed, and the highest quantum yield for the reduction of iron ($\Phi_{Fe(II)}$) was observed at pH 4.5 (Supporting Information, Figure S9). This phenomenon is also observed in other iron polycarboxylate systems, where the decrease in quantum yields at higher pHs is attributed to speciation of the Fe−carboxylate complex or precipitation as amorphous ferrihydrite.[37] On the basis of these results, the optimum pH for studying the quantum yield of the photoreaction was fixed at 4.5.

Our study showed remarkable differences for the $\Phi_{Fe(II)}$ of alginate and pectate systems: the photoreaction was much more efficient for alginate than for pectate, and this trend is also observed under anaerobic conditions, as shown in Table 1 and Figure S10 (Supporting Information).

Table 1. Measured Quantum Yields for the Photoreduction of Fe^{3+}[a]

Fe^{3+}−carboxylate	quantum yield ± SD
alginate	0.109 ± 0.005 (0.2523[b])
pectate	0.018 ± 0.005 (0.0416[b])
lactate	0.137 ± 0.002
pectate/lactate	0.013 ± 0.002
alginate/lactate	0.078 ± 0.005
citrate	0.211 ± 0.009
alginate/citrate	0.200 ± 0.006
β-hydroxybutyrate	0.009 ± 0.005

[a]$[Fe^{3+}]$ = 0.9 mM, [carboxylate] = 50 mM, [lactate] = 20 mM, [citrate] = 1.8 mM. [b]Measured in absence of molecular oxygen.

This sharp difference (≈1 order of magnitude) in quantum yields between alginate and pectate toward the reduction of Fe^{3+} was totally unexpected, and such a striking effect of the hydroxycarboxylate stereochemistry on the photochemical reactivity of a system had not been previously observed. The main difference between both polysaccharides is the stereochemistry of their building units; however, the functional groups in both materials are the same, and no significant difference is seen in the binding affinity of transition metal ions to either the G-blocks or M-blocks in alginate.[26]

In an effort to further identify the possible effect that the enantiomeric composition of these copolymers has on the quantum efficiency, we measured the $\Phi_{Fe(II)}$ for alginates with different mannuronate-to-guluronate ratios. For this purpose, alginate samples from different sources were analyzed by means of circular dichroism. This technique allowed estimating the M/G ratios by comparison of the peaks and troughs in the CD spectra, as reported in the literature.[43] Four alginate samples with different M/G compositions were used, and the results are reported in Table 2 (CD spectra are presented in the Supporting Information, Figure S11).

Table 2. Characterization and Measured Quantum Yields for Different Polyuronate Systems

polyuronate	$[\eta]$ (dL/g)	M_v (kDa)[a]	% M[b]	quantum yield[c]
alginate	2.2649	45	65.0	0.109
alginate-MV	5.2015 (2.0888)	110 (41)	61.0	0.0376 (0.0382)
alginate-AA	1.6920	33	59.8	0.0246
alginate-MVG	4.9433 (2.2733)	97 (45)	53.0	0.0130 (0.0195)
pectate	1.5466 (0.4262)	32 (12)	−[d]	0.017 (0.0090)

[a]Estimated using the Mark−Howink−Sakurada relationship and the respective constants published in the literature: Pectate,[44] $[\eta] = (1.4 \times 10^{-6})M^{1.34}$; alginate,[45] $[\eta] = 0.054M^{1}$ if 20 000 < M < 100 000 or $[\eta] = 0.0349M^{0.83}$ if 20 000 < M < 1 000 000. Values in parentheses correspond to hydrolyzed samples. [b]Calculated from circular dichroism measurements. [c]Determined by the 1,10-phenanthroline method. [d]Pectate is a homopolymer of galacturonnan and does not contain mannuronate units.

As shown in Table 2, those alginates containing a higher percentage of mannauronate showed the fastest photochemistry (highest $\Phi_{Fe(II)}$). Furthermore, hydrolysis of the studied polysaccharides afforded low molecular weight polymers, but the $\Phi_{Fe(II)}$ did not change accordingly. It is important to note that this is not a molecular weight or viscosity effect but trends with the higher M-block content, suggesting that it is the mannuronate-rich region that gives the highest photochemistry in alginates. The difference in composition in alginates also results in different gel morphology and porosity, as assessed by scanning electron microscopy (SEM). Micrographs presented in Figure S12 (Supporting Information) show an incremental increase in the average pore size as the percentage mannuronate increases. The morphology of the pores was studied in the internal region of the bead, immediately underneath the outer membrane, which did not present measurable pores at the used magnification (Supporting Information, Figure S12). The different organization of the polymeric chains during the gelation process reflects changes in the interaction of alginates with the Fe^{3+} ions in solution. These changes in the polymeric ligand−metal interaction could be the key to understanding the differences in photoreactivity. Interestingly enough, there seems to be a linear relationship between the reported quantum yields and the pore diameter in Fe−alginate gels, as presented in Figure S13 (Supporting Information).

To further elucidate the differences in photoreactivity of alginate vs pectate systems, the $\Phi_{Fe(II)}$ was determined for binary mixtures with different compositions in the two polysaccharides. The results indicate a power law dependence of the quantum efficiency, reaching a maximum when the molar fraction of alginate equals 1 (Supporting Information, Figure S14). This nonlinear behavior of the $\Phi_{Fe(II)}$ indicates that the chemical composition of individual sugar units might not be the most important factor affecting the photoreactivity in these systems, since the increase in molar fraction of the most reactive component (alginate), would be expected to yield a linear proportional increase in efficiency. The observed behavior suggests again a supramolecular component of the photoreaction: the coordination environment of the metal changes when the conformation of alginate is forced to change upon introduction of pectate chains in solution.

DOI: 10.1021/am506772x
ACS Appl. Mater. Interfaces 2015, 7, 3068−3076

In order to compare our systems with the Fe−alginate−lactate materials reported by Narayanan et al., the quantum yields for iron coordination complexes with different polycarboxylates were studied and are shown in Table 1. (This group first presented the system as photodegradable but did not report quantum yields for the reaction.) Addition of the lactate lowers the efficiency of the Fe^{3+}−alginate (Table 1). This lowering of the $\Phi_{Fe(II)}$ suggests that the mixed system is more stable than either the Fe^{3+}−lactate or Fe^{3+}−alginate alone. A different situation occurs when citric acid is added to the material: Even at low concentrations of citrate compared to the polyuronate (Fe:alginate:citrate was 1:50:2 mol ratio), the quantum yield rose, approaching that of the pure Fe^{3+}−citrate system (Table 1). This suggests that when the sacrificial acid is added, the photochemistry preferentially occurs between the metal and the citrate and the polysaccharide is not playing any significant role in the photochemical process but only in the physical gel-to-sol transition.

The effect of molecular oxygen on the photoreaction was evaluated for alginate and pectate by irradiating previously evacuated solutions under nitrogen atmosphere and comparing them with the aerobic samples. The presence of O_2 causes a decrease in the quantum yield for the production of Fe^{2+}, just as reported for iron−α-hydroxycarboxylic systems or for the well-known ferrioxalate, where oxygen reacts with the generated Fe^{2+}, oxidizing it back to Fe^{3+} with the formation of hydroperoxides and H_2O_2.[38]

Results indicate that the Fe^{3+}−polyuronate systems are less photoactive than the well-characterized iron α-hydroxycarboxylates[38,46] but much more reactive than iron β-hydroxybutirate, which we also analyzed for comparative purposes (Table 1). Polyuronic acids contain the 1—4 glycosidic linkage and they are not α-hydroxy acids but β,γ-dihydroxy acids. The reactivity of these systems is believed to be related to the presence of the ring oxygen in the vicinity of C-5, stabilizing the radical formed after decarboxylation.[47]

In order to study the structure−function relationships governing the photoreactivity of these polysaccharide complexes, we explored the role that the different functional groups present in these molecules play on the photochemical behavior. The structures of the studied polysaccharides and their derivatives are illustrated in Figure S15 (Supporting Information).

Initially, the photochemistry of potato starch, a polymer of glucose with no carboxylate groups, was evaluated in the presence of Fe^{3+} (Table 3). Although the sample absorbed light in the visible part of the spectrum, no photoreduction of iron was observed even at long irradiation times, which we hypothesize is due to the lack of interaction of Fe^{3+} with the hydroxyl groups of the polysaccharide at the working conditions.[48] If carboxylate groups are synthetically added by carboxymethylation of the above-mentioned starch, even at a degree of substitution as high as 20%, the photochemistry is still almost nonexistent, showing that the mere presence of a carboxylic acid function is not sufficient to ensure the photoreactivity of an Fe^{3+}−polysaccharide complex, and the stereochemistry and actual binding domain of the Fe^{3+} to the polysaccharide are playing a significant role (Table 3).

Table 3. Measured Quantum Yield for Starch and PUA Derivatives

product	DS[a]	$\Phi_{Fe(II)}$	product	DS[a]	$\Phi_{Fe(II)}$
potato starch		<0.001	CM pectate	0.15	0.009
CM starch	0.20	0.001	acetyl alginate	0.05	0.017
CM alginate	0.25	0.014	acetyl pectate	0.10	0.003

[a]DS: degree of substitution determined by ^{1}H NMR.

Protection of some of the −OH groups on alginate and pectate was done by acetylation and carboxymethylation reactions. In both cases, the quantum yields for the photoreduction of Fe^{3+} decreased markedly, even at low degrees of substitution (Table 3). This decrease in efficiency indicates that even if the hydroxyl groups themselves are not able to undergo any photochemistry with iron, as seen for potato starch, their presence in the sugar ring is somehow necessary for a more efficient photoreaction. These results suggest that the specific functional groups binding to the Fe^{3+} and the geometry of that binding play a significant role in determining the efficiency of the photoreaction.

3.2. Viscosity of Iron(III)−Polyuronate Systems. The effect of the Fe^{3+} loading on the rheological properties of these polysaccharides in solution was also studied. Capillary viscometry was first used to estimate the molecular weights of the alginate and pectate used for this study, and results are presented in Table 2.

Inherent viscosities of the system are plotted as a function of the iron-to-uronate unit ratio, as shown in Figure 2a. The viscosity in alginate solution initially decreases to reach a minimum when the metal-to-carboxylate ratio is around 1:0.15 and then constantly increases as more Fe^{3+} is added. In pectate, on the other hand, viscosity increases constantly with $[Fe^{3+}]$, sharply at the beginning, but at a lower rate when the ratio reaches 1:0.2; this difference in behavior might be due to the conformational properties of polygalacturonic acid, which has more character of an extended chain and presents much higher stiffness than alginate due to the higher degree of order along the polymeric chain.[49] Interestingly enough, even though pectate had a lower molecular weight than alginate and its solutions presented lower viscosities, once the iron was added to the system, the viscosities of Fe^{3+}−pectate solutions were always higher than the corresponding ones for alginate, with a higher molecular weight and a higher starting viscosity.

Irradiation of the samples with visible light caused a decrease in viscosity, as shown in Figure 2b. The weaker interaction with the photoproduced ferrous ions was already noticed for alginate gels,[24,25] and the reason can be explained by the high difference in lability that the two forms of iron have for water ligands, where Fe^{2+} is more labile than Fe^{3+}, resulting in much less stable complexes.[50] It is noticeable that Fe^{3+}−pectate samples suffer a bigger change in viscosity upon irradiation compared to alginate; however, the viscosity also decays more slowly, reaching the minimum at longer times, which is in agreement with our quantum yield measurements.

After exhaustively irradiating the coordination hydrogels, the resulting sol was demetalated, and the molecular weights of the samples were estimated from viscosity measurements. The molecular weights of both alginate and pectate decrease after irradiation (Supporting Information, Table S1), which is consistent with the breaking of the glycosidic linkages in the polysaccharide during the photoreaction. Although through a different mechanism, a similar behavior was reported for Eu(III)−alginate complexes, which showed a decrease in molecular weights upon UV light irradiation.[51]

3.3. Photochemistry in the Solid State. When irradiating Fe^{3+}−PUA xerogels under visible light, a discoloration of the

DOI: 10.1021/am506772x
ACS Appl. Mater. Interfaces 2015, 7, 3068−3076

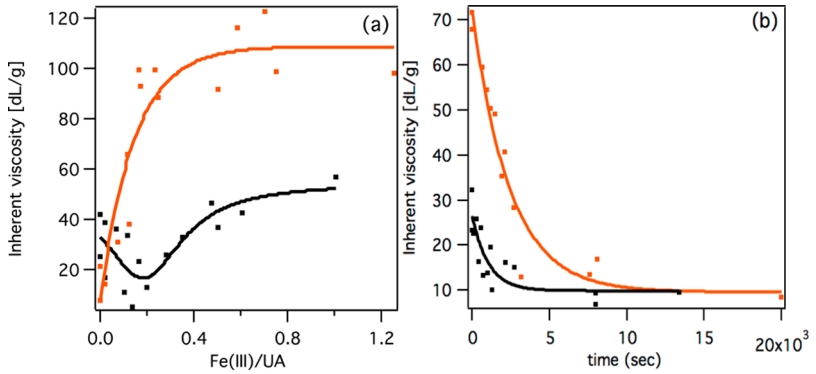

Figure 2. (a) Evolution of viscosity in alginate (black line) and pectate (orange line) solutions as Fe^{3+} concentration increased. (b) Decrease in inherent viscosities in iron−polyuronate samples upon irradiation at 405 nm. Fe:carboxylate was 1:0.46.

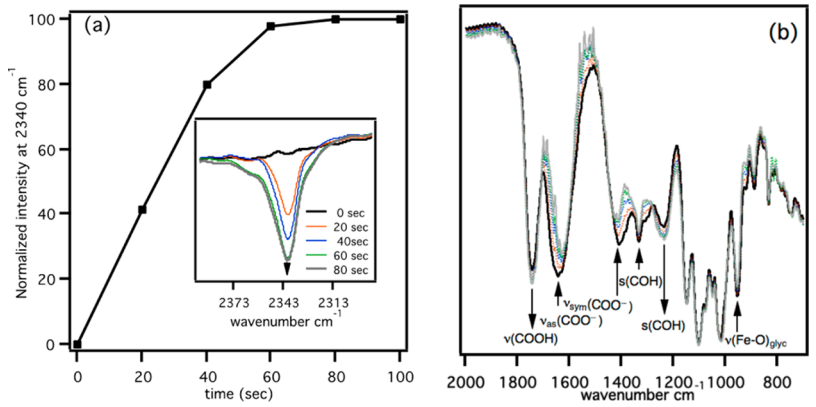

Figure 3. FTIR of an Fe^{3+}−pectate sample upon irradiation at 405 nm. (a) Evolution of the absorption band attributed to the carbon dioxide as the sample is photodecomposed. (b) Evolution of the rest of the signals upon irradiation.

exposed area was indicative of the reduction of the metal by light, even in the total absence of solvent. By preparing samples in KBr pellets and measuring the absorbance in the infrared after irradiation (Figure 3), the systematic evolution of CO_2 was observed from a strong absorption around 2342 cm^{-1}, confirming that the photochemistry in these systems goes through the decarboxylation of the polymer as the iron gets reduced. The absorption profile, which would normally show two main bands corresponding to two vibration modes of CO_2, in this case presents a unique signal due to the gas being tightly trapped inside the inorganic matrix and the rotational degrees of freedom being suppressed.[52] Decarboxylation upon irradiation was already observed in Eu^{3+}−polysaccharide systems, where the hydrophobization of the polymer was presented as indirect evidence.[51]

It is also important to notice that other signals in the spectrum are also changing as the photoreaction proceeds. That is the case of both $\nu_{as}(COO^-)$ and $\nu_{sym}(COO^-)$, the intensities of which decrease as the Fe^{3+} is converted to Fe^{2+}. Another important feature is the change in intensity of the signals at 1332 and 1230 cm^{-1}, corresponding to the stretching of C−OH bonds in the polysaccharide. Progressive changes are also observed for the band at 950 cm^{-1} assigned to the interaction between the metal and the glycosidic oxygen. This could be indicating that the coordination in Fe−polyuronate systems involves not only the carboxylate groups, but also the hydroxyl groups and the glycosidic moiety, as predicted by DFT calculations for other transition metal ion complexes with disaccharides.[26]

3.4. Photorelease from Iron(III)−PUA Beads. Hydrogel beads were prepared by ionotropic gelation, that is, using Fe^{3+} as a polyvalent cross-linker. A solid membrane forms instantaneously when the polysaccharide solution contacts the metal ion solution. Afterward, a compact bead is gradually formed as the metal diffuses from the exterior to the core of the capsule. To study the conditions for the formation of the beads, the concentration of the polysaccharide was fixed to 1% w/v and the concentration of iron was varied from 10 mM up to 0.1 M. Beads were mechanically stable only when the Fe^{3+} concentration was at least 30 mM and presented the highest mechanical stability when prepared in 0.1 M Fe^{3+}. In a complementary experiment, the concentration of Fe^{3+} was fixed at 0.1 mM and the concentration of PUA varied from 0.5% to 4% w/v. No beads were formed below 1% PUA, and the size of the beads was found to be dependent on the concentration of the polysaccharide (Supporting Information, Figure S16). For optimal bead size and mechanical properties in this study, hydrogel beads were prepared by keeping the concentration of the polysaccharide at 1% (50 mM) and the concentration of Fe^{3+} at 0.1 M.

By incorporating drug-model compounds into the polysaccharide solution before gelation, photoresponsive, loaded beads were formed. They were mechanically and chemically stable, hosting the cargo for long periods of time. However, not everything can be encapsulated; one must choose a molecule that is (1) bulky enough to be trapped inside the Fe^{3+}−PUA network and (2) photostable and nonreactive with other components of the formulation. Following this approach,

DOI: 10.1021/am506772x
ACS Appl. Mater. Interfaces 2015, 7, 3068−3076

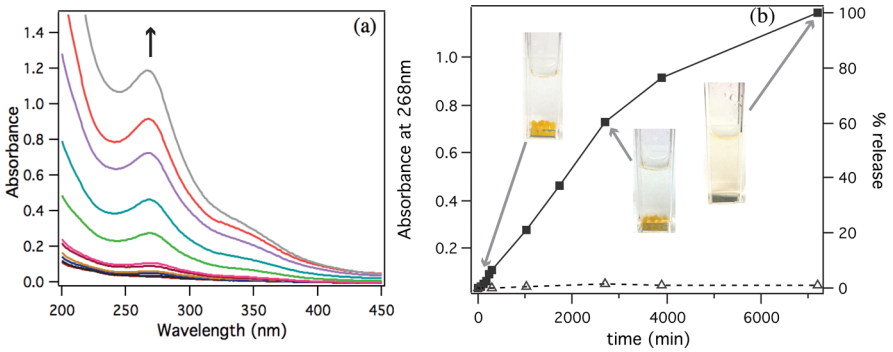

Figure 4. (a) Evolution of the absorption spectrum of the release medium upon irradiation of folic acid-loaded coordination gel beads with visible light and (b) release profile showing images of the beads at different irradiation times. The dotted line shows the changes in absorbance in the thermal control.

molecules as diverse as a dye (Congo Red), a vitamin (folic acid), and an antibiotic (chloramphenicol) were successfully encapsulated and photoreleased, as shown in Figures 4 and S17 (Supporting Information). By measuring changes in light absorption in the release media above the beads, the release of the encapsulated cargo upon irradiation was monitored [Figures 4 and S17 (Supporting Information)]. Also, a thermal control for all experiments was kept in the dark, showing in all cases a very low release of the cargo by thermal diffusion.

The efficiency of release of Congo Red was compared for both alginate and pectate beads (Supporting Information, Figure S18) and it parallels the efficiency of the photoreaction in aqueous solutions, where the alginate beads gave faster release compared to pectate ones. These beads were stable for long periods of time in the dark, even at 37 °C, in water and neutral buffers, as long as the buffer has a low ionic strength (Supporting Information, Figure S19a). Beads prepared in neutral water have been stable for longer than 5 months in the dark at room temperature (Supporting Information, Figure S19b)

In order to have an insight on the physical changes endured by the hydrogel beads during the irradiation process, SEM was used for analyzing the surface of the beads before and after irradiation. Micrographs presented in Figure 5 show how the

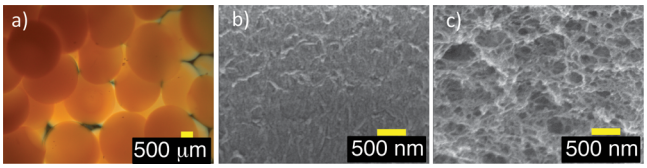

Figure 5. (a) Optical microscope image of Fe^{3+}–alginate beads prepared by ionotropic gelation, and SEM images showing changes in the surface of the beads before (b) and after (c) irradiation at 405 nm.

initially smoother surface of the bead becomes porous after light irradiation. The observed "Swiss-cheese" texture of the irradiated bead is presumably facilitating the effective release of the encapsulated cargo.

The photorelease of a load from these coordination hydrogel beads takes place as the Fe^{3+} bound to the polysaccharide gets photoreduced. The weaker interaction of ferrous ions with the polycarboxylate, in combination with the degradation of the polymer backbone as the decarboxylation proceeds, result in the eventual "dissolution" of the coordination gel, similar to that observed in the Fe/alginate/lactate gels.[25]

4. SUMMARY AND CONCLUSIONS

The photochemical reaction undertaken by Fe^{3+}–polyuronate coordination systems upon irradiation with visible light was quantitatively studied, and the principal characteristics of the reaction mechanism are reported. While the different PUAs studied in this paper present identic functional groups and differed only in the configuration of some chiral centers in the sugar units, the efficiency of the photoreaction showed itself to be largely dependent on the identity of the specific repetitive unit. Moreover, the efficiency of the reaction was independent of the molecular weight of the polysaccharide but sensitive to the pH. Fe^{3+}–PUA gels made with alginates with the highest M-character presented the highest quantum yields, and the photoreactivity trended with the M-composition. The microstructure of Fe^{3+}–alginate gels was studied and revealed relationships between the composition, the pore structure, and the quantum efficiency. This comparison of different Fe^{3+}–polysaccharides and quantitation of the photochemistry helps establishing guidelines to prepare Fe–sugar-based materials with different stabilities and photoreactivity. Furthermore, with choice of stereochemistry and modification of different functional groups, the photoreactivity of these systems can be tuned, thus giving ultimate control over the stability and responsiveness of the metal-coordination materials. Coordination hydrogel beads made from Fe–polyuronates show promise as drug-releasing vehicles at 37 °C in biological buffers and neutral aqueous solutions. Future work will focus on further modification of the polysaccharides to create new materials with different mechanical properties. With enhanced mechanical stability and tunable response to light, we envision creating new sugar-based metal-coordination materials that can be used as photoresponsive materials for a variety of applications.

■ ASSOCIATED CONTENT

Supporting Information

NMR spectra, CD spectra, quantum yield plots, chemical structures of derivatives, and release profiles. This material is available free of charge via the Internet at http://pubs.acs.org

■ AUTHOR INFORMATION

Corresponding Author

*E-mail: alexiso@bgsu.edu.

Author Contributions

The manuscript was written through contributions of all authors. All authors have given approval to the final version of the manuscript.

DOI: 10.1021/am506772x
ACS Appl. Mater. Interfaces 2015, 7, 3068–3076

Notes

The authors declare no competing financial interest.

■ ACKNOWLEDGMENTS

We thank Kimica Corp. for kindly providing Alginate MV and Alginate MVG samples. We thank Dr. Andy Torelli for aid with the CD. We also thank Dr. Marilyn Cayer for her assistance with SEM imaging. This work has been partially supported by a Building Strength FRC grant award from BGSU to A.D.O. (33000079) and by the Department of Chemistry start-up funding. C.T.S. acknowledges the BGSU CURS program for a summer research fellowship.

■ ABBREVIATIONS USED

QY = quantum yield
SEM = scanning electron microscopy
PUA = polyuronic acid
LMCT = ligand to metal charge transfer
CM = carboxymethyl
MCA = monochloroacetic acid
CD = circular dichroism.

■ REFERENCES

(1) Peppas, N. A.; Hilt, J. Z.; Khademhosseini, A.; Langer, R. Hydrogels in Biology and Medicine: From Molecular Principles to Bionanotechnology. *Adv. Mater.* **2006**, *18*, 1345−1360.
(2) Guarino, V.; Gloria, A.; Santis, R. D.; Ambrosio, L. Composite Hydrogels for Scaffold Design, Tissue Engineering, and Prostheses. In *Biomedical Applications of Hydrogels Handbook*; Ottenbrite, R. M., Park, K., Okano, T., Eds.; Springer: New York, 2010; pp 227−245.
(3) Jin, R.; Dijkstra, P. J. Hydrogels for Tissue Engineering Applications. In *Biomedical Applications of Hydrogels Handbook*; Ottenbrite, R. M.; Park, K.; Okano, T., Eds.; Springer: New York, 2010; pp 203−225.
(4) Weiss, P.; Fatimi, A.; Guicheux, J.; Vinatier, C. Hydrogels for Cartilage Tissue Engineering. In *Biomedical Applications of Hydrogels Handbook*; Ottenbrite, R. M., Park, K., Okano, T., Eds.; Springer: New York, 2010; pp 247−268.
(5) Zavan, B.; Cortivo, R.; Abatangelo, G. Hydrogels and Tissue Engineering. In *Hydrogels*; Springer: Milan, 2009; pp 1−8.
(6) Slaughter, B. V.; Khurshid, S. S.; Fisher, O. Z.; Khademhosseini, A.; Peppas, N. A. Hydrogels in Regenerative Medicine. *Adv. Mater.* **2009**, *21*, 3307−3329.
(7) Burdick, J. A.; Murphy, W. L. Moving from Static to Dynamic Complexity in Hydrogel Design. *Nat. Commun.* **2012**, *3*, 1269.
(8) Sun, J.; Tan, H. Alginate-Based Biomaterials for Regenerative Medicine Applications. *Materials* **2013**, *6*, 1285−1309.
(9) Vashist, A.; Vashist, A.; Gupta, Y. K.; Ahmad, S. Recent Advances in Hydrogel Based Drug Delivery Systems for the Human Body. *J. Mater. Chem. B* **2013**, *2*, 147−166.
(10) García, L.; Aguilar, M. R.; Román, J. S. Biodegradable Hydrogels for Controlled Drug Release. In *Biomedical Applications of Hydrogels Handbook*; Ottenbrite, R. M., Park, K., Okano, T., Eds.; Springer: New York, 2010; pp 147−155.
(11) Oh, K. S.; Yuk, S. H. Hydrogels-Based Drug Delivery System with Molecular Imaging. In *Biomedical Applications of Hydrogels Handbook*; Ottenbrite, R. M., Park, K., Okano, T., Eds.; Springer: New York, 2010; pp 179−200.
(12) Hoffman, A. S. Hydrogels for Biomedical Applications. *Adv. Drug Delivery Rev.* **2002**, *54*, 3−12.
(13) Buenger, D.; Topuz, F.; Groll, J. Hydrogels in Sensing Applications. *Prog. Polym. Sci.* **2012**, *37*, 1678−1719.
(14) Guenther, M.; Gerlach, G. Hydrogels for Chemical Sensors. In *Hydrogel Sensors and Actuators*; Gerlach, G., Arndt, K.-F., Eds.; Springer Series on Chemical Sensors and Biosensors; Springer: Berlin, 2010; pp 165−195.
(15) Appel, E. A.; Loh, X. J.; Jones, S. T.; Biedermann, F.; Dreiss, C. A.; Scherman, O. A. Ultrahigh-Water-Content Supramolecular Hydrogels Exhibiting Multistimuli Responsiveness. *J. Am. Chem. Soc.* **2012**, *134*, 11767−11773.
(16) Dong, H.; Snyder, J. F.; Williams, K. S.; Andzelm, J. W. Cation-Induced Hydrogels of Cellulose Nanofibrils with Tunable Moduli. *Biomacromolecules* **2013**, *14*, 3338−3345.
(17) Machida-Sano, I.; Matsuda, Y.; Namiki, H. In Vitro Adhesion of Human Dermal Fibroblasts on Iron Cross-Linked Alginate Films. *Biomed. Mater. (Bristol, U.K.)* **2009**, *4*, 025008.
(18) Machida-Sano, I.; Ogawa, S.; Ueda, H.; Kimura, Y.; Satoh, N.; Namiki, H. Effects of Composition of Iron-Cross-Linked Alginate Hydrogels for Cultivation of Human Dermal Fibroblasts. *Int. J. Biomater.* **2012**, *2012*.
(19) Guo, J. F.; Jourdian, G. W.; MacCallum, D. K. Culture and Growth Characteristics of Chondrocytes Encapsulated in Alginate Beads. *Connect. Tissue Res.* **1989**, *19*, 277−297.
(20) Munarin, F.; Petrini, P.; Tanzi, M. C.; Barbosa, M. A.; Granja, P. L. Biofunctional Chemically Modified Pectin for Cell Delivery. *Soft Matter* **2012**, *8*, 4731−4739.
(21) Liu, L.; Fishman, M. L.; Hicks, K. B. Pectin in Controlled Drug Delivery—A Review. *Cellulose* **2007**, *14*, 15−24.
(22) Ciofani, G.; Raffa, V.; Menciassi, A.; Micera, S.; Dario, P. A Drug Delivery System Based on Alginate Microspheres: Mass-Transport Test and in Vitro Validation. *Biomed. Microdevices* **2007**, *9*, 395−403.
(23) Qurrat-ul-Ain; Sharma, S.; Khuller, G. K.; Garg, S. K. Alginate-Based Oral Drug Delivery System for Tuberculosis: Pharmacokinetics and Therapeutic Effects. *J. Antimicrob. Chemother.* **2003**, *51*, 931−938.
(24) Jin, Z.; Güven, G.; Bocharova, V.; Halámek, J.; Tokarev, I.; Minko, S.; Melman, A.; Mandler, D.; Katz, E. Electrochemically Controlled Drug-Mimicking Protein Release from Iron−Alginate Thin-Films Associated with an Electrode. *ACS Appl. Mater. Interfaces* **2012**, *4*, 466−475.
(25) Narayanan, R. P.; Melman, G.; Letourneau, N. J.; Mendelson, N. L.; Melman, A. Photodegradable Iron(III) Cross-Linked Alginate Gels. *Biomacromolecules* **2012**, *13*, 2465−2471.
(26) Agulhon, P.; Markova, V.; Robitzer, M.; Quignard, F.; Mineva, T. Structure of Alginate Gels: Interaction of Diuronate Units with Divalent Cations from Density Functional Calculations. *Biomacromolecules* **2012**, *13*, 1899−1907.
(27) Barrett, D. G.; Fullenkamp, D. E.; He, L.; Holten-Andersen, N.; Lee, K. Y. C.; Messersmith, P. B. pH-Based Regulation of Hydrogel Mechanical Properties through Mussel-Inspired Chemistry and Processing. *Adv. Funct. Mater.* **2013**, *23*, 1111−1119.
(28) Piepenbrock, M.-O. M.; Lloyd, G. O.; Clarke, N.; Steed, J. W. Metal- and Anion-Binding Supramolecular Gels. *Chem. Rev.* **2009**, *110*, 1960−2004.
(29) Whittell, G. R.; Hager, M. D.; Schubert, U. S.; Manners, I. Functional Soft Materials from Metallopolymers and Metallosupramolecular Polymers. *Nat. Mater.* **2011**, *10*, 176−188.
(30) Urban, M. W. *Handbook of Stimuli-Responsive Materials*; John Wiley & Sons: New York, 2011.
(31) Fullenkamp, D. E.; He, L.; Barrett, D. G.; Burghardt, W. R.; Messersmith, P. B. Mussel-Inspired Histidine-Based Transient Network Metal Coordination Hydrogels. *Macromolecules* **2013**, *46*, 1167−1174.
(32) Chen, X.; Wang, S.; Lu, M.; Chen, Y.; Zhao, L.; Li, W.; Yuan, Q.; Norde, W.; Li, Y. Formation and Characterization of Light-Responsive TEMPO-Oxidized Konjac Glucomannan Microspheres. *Biomacromolecules* **2014**, *15*, 2166−2171.
(33) Davis, T. A.; Llanes, F.; Volesky, B.; Diaz-Pulido, G.; McCook, L.; Mucci, A. 1H-NMR Study of Na Alginates Extracted from Sargassum Spp. in Relation to Metal Biosorption. *Appl. Biochem. Biotechnol.* **2003**, *110*, 75−90.
(34) Balsamo, V.; López-Carrasquero, F.; Laredo, E.; Conto, K.; Contreras, J.; Feijoo, J. L. Preparation and Thermal Stability of Carboxymethyl Starch/Quaternary Ammonium Salts Complexes. *Carbohydr. Polym.* **2011**, *83*, 1680−1689.

DOI: 10.1021/am506772x
ACS Appl. Mater. Interfaces 2015, 7, 3068−3076

(35) Li, X.; Xu, A.; Xie, H.; Yu, W.; Xie, W.; Ma, X. Preparation of Low Molecular Weight Alginate by Hydrogen Peroxide Depolymerization for Tissue Engineering. *Carbohydr. Polym.* **2010**, *79*, 660−664.
(36) Frahn, J. The Photochemical Decomposition of the Citrate-Ferric Iron Comples: A Study of the Reaction Products by Paper Ionoporesis. *Aust. J. Chem.* **1958**, *11*, 399−405.
(37) Feng, W.; Nansheng, D. Photochemistry of Hydrolytic Iron(III) Species and Photoinduced Degradation of Organic Compounds. A Minireview. *Chemosphere* **2000**, *41*, 1137−1147.
(38) Faust, B. C.; Zepp, R. G. Photochemistry of Aqueous Iron(III)−Polycarboxylate Complexes: Roles in the Chemistry of Atmospheric and Surface Waters. *Environ. Sci. Technol.* **1993**, *27*, 2517−2522.
(39) Amin, S. A.; Green, D. H.; Küpper, F. C.; Carrano, C. J. Vibrioferrin, an Unusual Marine Siderophore: Iron Binding, Photochemistry, and Biological Implications. *Inorg. Chem.* **2009**, *48*, 11451−11458.
(40) Barbeau, K.; Zhang, G.; Live, D. H.; Butler, A. Petrobactin, a Photoreactive Siderophore Produced by the Oil-Degrading Marine Bacterium *Marinobacter hydrocarbonoclasticus*. *J. Am. Chem. Soc.* **2002**, *124*, 378−379.
(41) Šima, J.; Makáňová, J. Photochemistry of Iron(III) Complexes. *Coord. Chem. Rev.* **1997**, *160*, 161−189.
(42) Pozdnyakov, I. P.; Wu, F.; Melnikov, A. A.; Grivin, V. P.; Bazhin, N. M.; Chekalin, S. V.; Plyusnin, V. F. Photochemistry of Iron(III)−Lactic Acid Complex in Aqueous Solutions. *Russ. Chem. Bull.* **2013**, *62*, 1579−1585.
(43) Morris, E. R.; Rees, D. A.; Thom, D. Characterisation of Alginate Composition and Block-Structure by Circular Dichroism. *Carbohydr. Res.* **1980**, *81*, 305−314.
(44) Catoire, L.; Derouet, C.; Redon, A.-M.; Goldberg, R.; Hervédu Penhoat, C. An NMR Study of the Dynamic Single-Stranded Conformation of Sodium Pectate. *Carbohydr. Res.* **1997**, *300*, 19−29.
(45) Vold, I. M. N.; Kristiansen, K. A.; Christensen, B. E. A Study of the Chain Stiffness and Extension of Alginates, in Vitro Epimerized Alginates, and Periodate-Oxidized Alginates Using Size-Exclusion Chromatography Combined with Light Scattering and Viscosity Detectors. *Biomacromolecules* **2007**, *8*, 2627−2627.
(46) Balzani, V.; Moggi, L. Photochemistry of Coordination Compounds: A Glance at Past, Present, and Future. *Coord. Chem. Rev.* **1990**, *97*, 313−326.
(47) Stapley, J. A.; BeMiller, J. N. The Hofer−Moest Decarboxylation of D-Glucuronic Acid and D-Glucuronosides. *Carbohydr. Res.* **2007**, *342*, 610−613.
(48) Somsook, E.; Hinsin, D.; Buakhrong, P.; Teanchai, R.; Mophan, N.; Pohmakotr, M.; Shiowatana, J. Interactions between Iron(III) and Sucrose, Dextran, or Starch in Complexes. *Carbohydr. Polym.* **2005**, *61*, 281−287.
(49) Braccini, I.; Grasso, R. P.; Pérez, S. Conformational and Configurational Features of Acidic Polysaccharides and Their Interactions with Calcium Ions: A Molecular Modeling Investigation. *Carbohydr. Res.* **1999**, *317*, 119−130.
(50) Bertini, I. *Biological Inorganic Chemistry: Structure and Reactivity*; University Science Books: Sausalito, CA, 2007.
(51) Okajima, M. K.; le Nguyen, Q. T.; Tateyama, S.; Masuyama, H.; Tanaka, T.; Mitsumata, T.; Kaneko, T. Photoshrinkage in Polysaccharide Gels with Trivalent Metal Ions. *Biomacromolecules* **2012**, *13*, 4158−4163.
(52) Keresztury, G.; Incze, M.; Sóti, F.; Imre, L. CO_2 Inclusion Bands in I.R. Spectra of KBr Pellets. *Spectrochim. Acta, Part A* **1980**, *36*, 1007−1008.

DOI: 10.1021/am506772x
ACS Appl. Mater. Interfaces 2015, 7, 3068−3076